

# **Pricing Derivatives With Modeling CO<sub>2</sub> Emission Allowance Using a Regime Switching Jump Diffusion Model : With Regime-Switching Risk Premium**

Son-Nan Chen<sup>a</sup>

Shih-Kuei Lin<sup>b</sup>

Chang-Yi Li<sup>c</sup>

- 
- a. Professor of Finance at Shanghai Advanced Institute of Finance, Shanghai Jiatong University, Shanghai, China 200030, and can be reached at +86-21-62933418 (fax), or snchen@saif.sjtu.edu.cn
  - b. Associate Professor of Finance at Department of Money and Banking, National Chengchi University, Taipei, Taiwan, and can be reached at +886-2-29398004 (fax), or square@nccu.edu.tw
  - c. a Ph.D. candidate at Department of Money and Banking, National Chengchi University, Taipei, Taiwan, and can be reached at +886-2-29398004 (fax), or archakea@gmail.com

## Abstract

The European Union Emissions Trading Scheme (EU ETS) is one of the most important initiatives ever taken to limit the greenhouse gas emissions that cause climate change. Carbon markets trade with the spot European Union Allowance (EUA), with one EUA providing the right to emit one tone of Carbon dioxide ( $\text{CO}_2$ ). We examine the spot EUA returns in BlueNext that exhibit a volatility clustering feature and the carbon-market system that is impacted by the announcements of  $\text{CO}_2$  emissions policies. We propose a regime-switching jump diffusion model (RSJM) with a hidden Markov chain to capture not only a volatility clustering feature, but also the dynamics of the spot EUA returns that are influenced by change in the  $\text{CO}_2$  emissions policies, and thereby altering jump arrivals. Thus, the carbon-market macroeconomic environment affects the switching intensities of the RSJM. We derive the theoretical futures-option prices with a stochastic convenience yield under a jump diffusion model (JDM) and the RSJM via the generalized Esscher transform on two sets of filtration that carry a regime-switching risk premium under the carbon-market environment. The empirical study shows that the derived futures-option prices exhibit the best performance under the RSJM.

**Key word:** European Union Emissions Trading Scheme; Markov modulated Poisson process; Esscher transform; Black's formula; Jump diffusion model.

## 1. Introduction

Since the industrial revolution originated in Britain in the eighteenth century, human beings have excessively relied on petrochemical products, including the burning of fossil fuels. Carbon dioxide (CO<sub>2</sub>) emissions and the greenhouse gas have led directly to climate change, and thereby causing extreme environmental changes such as an increasing frequency of hurricanes, droughts and floods, colder or hotter weather. In addition, it also causes human lives and a huge loss of properties. As a result, many countries and organizations have taken measures to reduce CO<sub>2</sub> to lessen the effect of extreme climate changes. The Kyoto Protocol, the most crucial international commitment, was stipulated in 2008 for lowering greenhouse gases CO<sub>2</sub>, and thus carbon markets were born for the purpose of reducing CO<sub>2</sub> emissions.

The carbon trading markets are divided into two categories of carbon products. One is the carbon trading program, including the European Union Emissions Trading (EU ETS), the New South Wales (NSW), the Chicago Climate Exchange (CCE), the Regional Greenhouse Gas Initiative (RGGI), and the Assigned Amount Units (AAU). The other is the greenhouse-gas reduction project in Kyoto Protocol, including the Clear Development Mechanism (CDM), the Joint Implementation and the voluntary market. Table 1 reports the evolution of the trading value of EU ETS allowances in the carbon markets from 2005 to 2010. Other allowances in Table 1 involve the trading carbon value in NSW, CCE, RGGI, and AAU, and other offsets cover the Joint Implementation and the voluntary market. As observed, the trading value of EUAs increased substantially from 2005 to 2010, and EUAs accounted for 84 percent in value of the global carbon market in 2010.

【Insert Table 1 】

There are some differences between the carbon markets of the EU ETS and the financial markets in terms of the provisions of cap-and-trade, the characteristic of different periods, and the largest existing emission-trading scheme for the spot EUAs. Seifert et al. (2008) present a tractable stochastic equilibrium model to reflect the stylized features of the EU ETS, including the largest existing emission-trading scheme, penalty costs, banking and borrowing, the trading period break, and increasing marginal abatement costs, and then use the model to analyze the CO<sub>2</sub> spot price dynamics. They find that CO<sub>2</sub> prices do not follow any seasonal pattern, and discounted prices should possess the martingale property. They conclude that an adequate CO<sub>2</sub> price process should exhibit a time- and price- dependent volatility structure.

Hinz and Novikov (2010) explain the logical principles underlying the risk-neutral modeling of emission certificate price evolution, and show that, within a realistic situation of a risk-averse market equilibrium, there is a useful feedback relation characterizing risk. The presence of jump events is particularly important to describe price shocks, which may be induced by possible discontinuities in information flow. Moreover, Borovkov et al. (2010) extend the Hinz-Novikov model by assuming the emission allowance certificates to follow a jump-diffusion model under the continuous-time framework. Carmona et al. (2009) investigate a dynamic price equilibrium and provide a mathematical analysis of market equilibrium and an optimal stochastic control that shows social optimality. In addition, Cetin (2009) consider the different stages of the spot EUAs using a Markov chain in the local risk minimization to examine evaluation and hedging.

Daskalakis et al. (2009) investigate three main markets for the spot EUAs within the EU ETS: Powernext<sup>1</sup>, Nord Pool and European Climate Exchange (ECX), and suggest that the prohibition of banking emission allowances between distinct phases of the EU ETS has a significant implication in terms of futures pricing. They develop both theoretically and empirically a valid framework for pricing and hedging options on intra-phase and inter-phase futures. Uhrig-Homburg and Wagner (2009) study the relationship between the spot EUAs and the EUAs futures, and find that the EUAs futures are the price discovery processes of the spot EUAs. However, it is important to note that due to the market design, the first- and the second-period (called Phase I and Phase II, here-after) spot EUAs are just two different goods. Therefore, the link between the first-phase spot and the second-phase futures is naturally very weak. Benz and Trück (2009) study Markovian and AR-GARCH models to fit the return of spot EUAs from EU ETS. In addition, Cetin and Verschuere (2010) employ a hidden Markovian process and a filtering approach to capture the impact of news release, and derive the option pricing models within the EU ETS.

Daskalakis et al. (2009) find that a jump diffusion model (JDM), proposed by Merton (1976), provides a better fit to the return of the spot EUAs than other models. However, we find that there is a volatility clustering feature in the return of the spot EUAs, which cannot be captured by the JDM. Hence, we propose a RSJM with regime-switching intensities of jump to capture the dynamics of the spot EUAs returns which are influenced by change in the macroeconomic condition of the carbon market and the policies released from EU ETS. Moreover, the theoretical futures-option prices are derived under the JDM and the RSJM via the generalized

---

<sup>1</sup> On 21/12/2007, NYSE Euronext purchased the environmental business lines of Powernext, which launched a new market in Paris under the name BlueNext.

Esscher transform on two kinds of filtration. We find that the RSJM not only produces the result consistent with the volatility clustering feature, but also provide more accurate theoretical futures and futures-option prices. In addition, the RSJM is able to detect the existence of regime switching risk. We also compare the accuracy of the theoretical futures-option prices under the Black' formula, the JDM and the RSJM with a constant and a stochastic convenience yield.

This article is organized as follows: Section II describes the EU emissions trading carbon emission allowances using a statistic description and an economic analysis for BlueNext. In Section III, we investigate three models such as the Black-Scholes model (BSM), the JDM and the RSJM. The pricing formulas of futures and futures options under the EU ETS are derived in Section IV. Section V provides an empirical analysis of the futures options. The final section concludes the results.

## **2. Economic analysis of EUAs in the EU ETS**

This section investigates the dynamics of the spot EUAs, the EUA futures and the futures options using economic and policy analysis, and also show, based on the past data, how abnormal price is changed in the carbon market. The spot emission allowances in Europe are mainly traded through two largest spot EUAs markets, the BlueNext and the European Energy Exchange (EEX). In 2009, the BlueNext exchange accounted for almost 63% of the spot market transactions in the EU ETS market, while the EEX was about 16%. The data used in this study consist of the daily closing prices for the period 24/06/2005-28/12/2007 and 26/02/2008-30/12/2010 at the BlueNext. Panel A and B in Figure 1 represent, respectively, the daily closing prices and the return dynamics of spot EUAs in the BlueNext market.

## 【Insert Figure 1】

According to the enforcement of the Kyoto Protocol in 2008, the dynamics of the EU ETS is divided into three phases (Alberola et al. 2008; Chevalier, 2009 and 2010; Denny et al. 2010): the first phase (Phase I) represents the previous Kyoto Protocol era from 2005 to 2007, Phase II denotes the Kyoto Protocol era from 2008 to 2012, and Phase III indicates the Post-Kyoto Protocol era from 2013 to 2020. In Phase II, the European Union target for the then fifteen member states was set a reduction of 8 % below the 1990 emissions level. The target in Phase III was a reduction of 21% lower than the 2005 level. In the three phases, the dynamics, the statistics and the characteristics of the price of spot EUAs are described sequentially as follows.

### **Phase I: Previous Kyoto Protocol Era (2005-2007)**

The EU ETS started on January 1, 2005. Phase I was introduced as a warm-up period and it was operated in this phase to put in place the policies infrastructure of permit trading. From the beginning of €8/ton on January 1, 2005, spot EUAs prices rose to €25-30/ton until the release of the 2005 verified emission on April 24, 2006, which caused a depressive effect on the spot EUAs prices as shown in Figure 1 by a sharp break in the spot EUAs price. Based on this sharp break, Alberola et al. (2008) divided Phase I into two periods, Period I from 24/06/2005 to 24/04/2006 and Period II from 01/06/2006 to 28/12/2007. Based on the BlueNext data, some economic features in spot EUAs are given as follows.

#### **Period I in Phase I: Demand over Supply**

In this period, the spot EUAs price began with 8€/ton on January 1, 2005, and

increased to around 30€/ton in July 2005, which fluctuated in a range of 20-25€/ton for almost the following six months, and then rose to 30€/ton. The demand came mainly from power producers, while most of other market participants did not take advantage of buying/selling carbon allowances. In addition, the demand for the spot EUAs continued to expand primarily from power operators, and increased substantially during the winter due to a rise in energy prices, especially in gas price (Alberola et al. 2008; Kanen, 2006; Christiansen et al. 2005; Bunn and Fezzi, 2007; Convery and Redmond, 2007; Mansanet-Bataller et al. 2007). Thus, the main driver of price jumps came from carbon prices in Period I. Table 2 reports that 11 jump events are recorded in Period I when the  $\pm 5\%$  excess returns in spot EUAs are regarded as jump events.

**【Insert Table 2】**

### **Period II in Phase I: Excess of Supply over Demand**

In the final week of April 2006, the spot EUAs prices collapsed when power operators disclosed the 2005 verified emission data showing that there was an oversupply of the spot EUAs. And then its prices moved in the range from 15€/ton to 20€/ton until October 2006 (Alberola et al. 2008). In addition to the oversupplied 2005 verified emission, the prices in Period II declined toward zero due to the banking restrictions that the allowances distributed in Phase I were not valid in Phase II. However, during Phase II and III, EUAs were fungible between the different phases. Therefore, change in the policy issue such as the oversupplied verified emission and the banking restrictions is the main driver of a decrease in the spot EUAs toward zero, which leads to price jumps in carbon price in Period II. The

carbon-price driver is evidenced to vary with institutional events such as emissions cap and the banking restrictions (Alberola et al. 2008). Table 2 reports that 147 jump events are recorded in Period II when the  $\pm 5\%$  excess returns in the spot EUAs are considered as jump events, and about two thirds of the total jump events are identified as decreasing jump events.

### **Phase II: Kyoto Protocol Era (2008-2012)<sup>2</sup>**

In Phase II, spot EUAs prices increase to 20€/ton primarily because the European Commission has reaffirmed that it will enforce tighter targets. During Phase I, if an installation does not meet its emission target during the year, the penalty is equal to 40€/ton in excess, plus the restitution of one allowance in the following year. During Phase II, the penalty is increased to 100€/ton, following the same principle. Carbon prices in Phase II have been more stable and healthy in the price pattern compared to Phase I. As shown in Figure 1, the CO<sub>2</sub> price has been oscillating between 10€/ton and 30€/ton, depending on the levels of allowances demand due to industrial production and the depressive impact of the economic crisis. Therefore, the jump events are primarily driven by business activity and the financial tsunami in Phase II. Table 2 reports 34 jump events in Phase II when the  $\pm 5\%$  excess returns in the spot EUAs are identified as jump events.

Christiansen et al. (2005) and Alberola et al. (2008) have identified the main drivers of the carbon price as policies issues, energy prices, temperature events and

---

<sup>2</sup> South Africa hosted the 17<sup>th</sup> Conference of Parties of the United Nations Framework Convention on Climate Change (UNFCCC COP 17) in 2011. There are two important results from the UNFCCC COP 17 climate summit in Durban. First, the Kyoto Protocol will be on life support until it is replaced by a new agreement. Secondly, Ad Hoc Working Group on the Durban Platform for Enhanced Action will have a protocol, legal instrument or agreed outcome with legal force after 2020.

economic activity, which also cause the carbon price to jump. By observing the number of the spot-EUAs jump events in Phase II and in Period I and II of Phase I, the arrival rates of jumps vary with different periods. Therefore, to identify a suitable model for the dynamic behavior of the spot EUAs and their derivatives, we analyze the performance of the BSM, the JDM, and the RSJM in the following sections.

### 3. Financial and econometric analysis of emission allowances

In this section, we introduce the properties and characteristics of the three models, the BSM, the JDM and the RSJM. We also provide a parameter-estimation method along with the relevant literature. Then, the carbon emission allowances are tested with the three proposed models in the BlueNext exchange. Finally, we show that the characteristics of the carbon emissions-allowances markets are consistent with the result obtained from the RSJM.

#### 3.1 Black-Scholes model

The Black-Scholes model (1973, BSM) is widely used for the valuation of options and options on futures. Under the BSM, the dynamics of the spot EUAs  $S(t)$  is described by a geometric Brownian motion process given below,

$$\frac{dS(t)}{S(t)} = \mu dt + \sigma dW(t) \quad (1)$$

where  $\mu$  denotes the instantaneous mean return at time  $t$ ,  $\sigma$  is the volatility of the instantaneous return, and  $W(t)$  is a Brownian motion. By Itô's Lemma, the logarithmic return can be written by the following equation,

$$R_B(t) = \bar{\mu} + \sigma \mathcal{N} \quad (2)$$

where  $R_p(t)$  is the logarithmic return at time  $t$  and  $\bar{\mu}$  denotes the mean of the logarithmic return at discrete time  $\Delta t$ .  $\mathcal{N}$  is a normal distribution with zero mean and variance  $\Delta t$ .

Fama (1965) provides a strong evidence in favor of the random-walk hypothesis and the leptokurtic behavior of the stock price. Mandelbrot (1963) finds that the “stable Paretian” distribution is better than a normal distribution to fit the skewness and kurtosis features of the underlying asset return. Kou (2002) also shows that the BSM cannot capture the leptokurtosis in the dynamic behavior of the stock return and volatility smile observed in option markets. Merton (1976) and Kou (2002) also propose a JDM to address the skewness and kurtosis found in the observed behavior of the stock return and volatility smile.

### 3.2 Jump diffusion model

Merton (1976) develops a jump diffusion model (JDM) to represent the continuous process of asset returns with a Brownian motion and a discontinuous variation with a compound Poisson process. By following the JDM, the dynamics of the spot EUAs price can be described by (3) given below,

$$\frac{dS(t)}{S(t-)} = \mu dt + \sigma dW(t) + d \left( \sum_{n=1}^{N(t)} (e^{Z_n} - 1) \right) \quad (3)$$

where  $\mu$  and  $\sigma$  denote, respectively, the mean return and the return volatility conditional on no jump events occurred. The term,  $\sum_{n=1}^{N(t)} (e^{Z_n} - 1)$ , represents a compound Poisson process.  $N(t)$  is a Poisson process with mean jump  $\lambda t$  over a

time period from 0 to  $t$ , and the jump variable,  $Z_n = \ln \frac{S(t)}{S(t-)}$ , has a normal distribution with mean  $\mu_j$  and variance  $\sigma_j^2$ . By using the Itô-Doléans formula, the return dynamics of the spot EUAs can be rewritten as follows,

$$R_j(t) = \bar{\mu} + \sigma \mathcal{N} + \sum_{n=1}^{N(t)} Z_n \quad (4)$$

where  $\sum_{n=1}^{N(t)} Z_n$  denotes a compound Poisson with a discontinuous time  $\Delta t$ .

A volatility clustering phenomenon explored by Mandelbrot (1963) essentially implies that large volatility is subsequently followed by large one and small volatility succeeded by small one. Kou (2002) points out that the JDM can neither capture clustering fluctuations nor address the volatility clustering feature in stock returns. This feature is also observed in the carbon-market returns, when relevant information comes along with a high frequency for a period of time or a low frequency for another period. Daskalakis et al. (2009) find that, by using statistical tests, the JDM is better to capture the dynamics of the spot EUAs return than other models such as the Geometric Brownian motion model (GBM), the mean-reverting square-root model (MRSRM), the mean-reverting logarithmic model, the model of constant elasticity of variance, the GBM with jump risk, and the MRSRM with jump risk. However, the jump diffusion model cannot accommodate for volatility clustering. Therefore, we use a regime-switching jump diffusion model to fit the observed return of the spot EUAs and to capture the volatility clustering feature.

### 3.3 Regime switching Jump diffusion model

We propose a regime-switching jump diffusion model (RSJM) to capture the

leptokurtic return feature, volatility smile, and volatility clustering by a Markov chain with two intensities. More precisely, the dynamics of the spot EUAs price is given by

$$\frac{dS(t)}{S(t-)} = \mu dt + \sigma dW(t) + d \left( \sum_{n=1}^{\Phi(t)} (e^{Z_n} - 1) \right) \quad (5)$$

where  $\Phi(t)$  denotes a Markov-modulated Poisson process with Markov process  $X(t)$  having a finite state space  $I = \{1, 2\}$ , and  $Z_n$  represents an independent sequence of jump sizes which are normally identically distributed with mean  $\mu_j$  and variance  $\sigma_j^2$ . Assume that the state of the carbon market is a homogeneous continuous-time hidden Markov chain  $X = \{X(t)\}$ . The transition matrix can be written as follows

$$P^c(t) = \begin{bmatrix} p_{11}(t) & 1 - p_{11}(t) \\ 1 - p_{22}(t) & p_{22}(t) \end{bmatrix} = e^{\Psi t} \quad (6)$$

where  $\Psi = \begin{bmatrix} -\alpha_1 & \alpha_1 \\ \alpha_2 & -\alpha_2 \end{bmatrix}$  denotes a transition-rate matrix,  $\alpha_i, i=1,2$  represents the

transition rate leaving from state  $i \in I$  to the other state, and  $-\alpha_i$  is the transition

rate arriving from the other state to state  $i$ .  $(\pi_1, \pi_2) = \frac{1}{\alpha_1 + \alpha_2} (\alpha_2, \alpha_1)$  denote the

initial stationary states of  $X(0)$ . Assume that  $(\Omega, \mathcal{F}, \mathbb{P})$  is a complete probability

space. Let  $X(t)$  and  $\Phi(t)$  be defined by the joint probability,

$P_{ij}(n, t) \equiv \mathbb{P}(X(0) = i, X(t) = j, \Phi(t) = n)$ , under the Markov modulated Poisson

process. A Laplace transformation of the Markov-modulated Poisson process is

defined as  $P_{ij}(\xi, t) = \sum_{n=0}^{\infty} P_{ij}(n, t) \xi^n$ ,  $\forall 0 \leq \xi \leq 1$  (cf. Last and Brandt, 1995). Under

the Kolmogorov's forward equation, the moment generating function has a unique solution for  $\mathbf{P}(\xi, t) = \exp[(\Psi - (1 - \xi)\Lambda)t]$ , where  $\Lambda$  is an intensity matrix

$$\begin{bmatrix} \lambda_1 & 0 \\ 0 & \lambda_2 \end{bmatrix} \quad \text{and} \quad \exp(A) = \sum_{n=0}^{\infty} \frac{A^n}{n!} \quad \text{where } A \text{ is a square matrix.}$$

Similarly, by using the Itô-Doléans formula and simplifying the transition of the states, the return dynamics of the spot EUAs can be rewritten by

$$R_R(t) = \bar{\mu} + \sigma \mathcal{N} + \begin{cases} \sum_{n=1}^{N_1(t)} Z_n & \text{if } X(t) = 1 \\ \sum_{n=1}^{N_2(t)} Z_n & \text{if } X(t) = 2 \end{cases} \quad (7)$$

where  $N_i(t)$  denotes a Poisson process with intensity  $\lambda_i$  for time period  $\Delta t$  in state  $i \in \{1, 2\}$ . Here, the transition matrix of (7) can be denoted similarly as (6) and given below:

$$P^d(\Delta t) = \begin{bmatrix} p_{11}(\Delta t) & 1 - p_{11}(\Delta t) \\ 1 - p_{22}(\Delta t) & p_{22}(\Delta t) \end{bmatrix} = \begin{bmatrix} p_{11} & 1 - p_{11} \\ 1 - p_{22} & p_{22} \end{bmatrix}. \quad (8)$$

Next, we estimate the parameters of the discrete models described in (2), (4), (7) and (8), and test empirically the BSM, the JDM, and the RSJM using the maximum likelihood (LR) estimation and the likelihood ratio test (LRT). The RSJM parameters are estimated using the maximum likelihood method with the Expectation Maximization algorithm (EM, Dempster et al. 1977) and a gradient algorithm (Lange, 1995). Their standard deviations are estimated using Supplemented Expectation

Maximization algorithm (SEM, Meng et al. 1991). We shall show that both the regime and the jump dynamics of the spot EUAs returns can produce the result that is consistent with the empirical phenomenon exhibited in Phase I and II. Then, we check whether or not the RSJM can capture the volatility clustering feature by using the autocorrelation of squared spot EUAs returns.

### 3.4 Empirical analysis

The model parameters are estimated via the EM using the spot EUAs price data from the BlueNext from 24/06/2005 to 30/12/2010. The parametric estimators and the statistical test are listed in Table 3 for the three models: the BSM, the JDM, and the RSJM. The mean ( $\bar{\mu}$ ) and the standard deviation ( $\sigma$ ) of the BSM are, respectively, 0.0011 and 0.0251 in Period I, and -0.0163 and 0.924 in Period II of Phase I. The spot EUAs price increases in Period I while decreasing in Period II. In addition, the spot EUAs price is more volatile in Period II than in Period I. The LR test results show rejecting the BSM at the 95% significance level, which is consistent with Daskalakis et al. (2009) who find that the JDM is better than other competing models. In addition, the jump frequency ( $\lambda_1$ ), the mean ( $\mu_j$ ) and the volatility ( $\sigma_j$ ) of the logarithmic jump size of the JDM are, respectively, 0.4846, -0.0026 and 0.0314 in Period I, and 0.9789, -0.1710 and 0.0879 in Period II. The jump frequency of the spot EUAs price increases from Period I to Period II, while the mean and the volatility of the logarithmic size are downward with a variation from Period I to Period II.

【Insert Table 3 】

Further, in Table 3 based on the LR tests of the three models in Phase I, the JDM

is found to be a better fit than the BSM (the LRT 632.38 is significant at the 95% level), and the RSJM is better than the JDM (the LRT 134.21 is significant at the 95% level). Thus, the RSJM is the best performer among the three models. With the RSJM, the transition probabilities  $p_{11}$  and  $p_{22}$  in Phase I are, respectively, 0.9868 and 0.9830. These two high transition probabilities imply that the probability of switching from a low frequency (0.0009) to a high frequency (1.0460) is very small, and vice versa. In addition, the Carbon price drivers in Phase I tend to vary depending on institutional events such as emissions cap and banking restrictions, which in turn affect the frequencies of information arrivals for good or bad news. Finally, Table 3 also shows by the LR test results that the RSJM in Phase II provides a better fit than the JDM (the LRT 79.89 is significant at the 95% level). The above RSJM test results carry over to Phase II.

Figure 2 plots the dynamics of the spot EUAs price, its logarithmic return, the probability of low frequency, and the probability of jumps in Phase II. By observing Panel A, during the financial crisis started to occur in July, 2008, the spot EUAs prices went down because the CO<sub>2</sub> emissions were low in industrial production. Panel B reveals the fact that the volatility was higher in 2008 than in 2009 and 2010, implying that the jump frequency was higher in 2008. In addition, Panel B also provides an evidence of volatility clustering, while Panel C indicates a high probability of low frequency from February, 2008 to July, 2008, owing to the new CO<sub>2</sub> emission policies, and also a low probability of low frequency from October, 2008, to June, 2009 which was caused by the financial crisis that led to a decrease in the CO<sub>2</sub> emissions. Hence, there was a transition of states from a low frequency to a high frequency in October, 2008 and from a high frequency to a low frequency in

June, 2009. As the financial crisis almost fully developed in around October, 2008, the probability of a low (high) frequency became lower (higher). In addition, there was also a switch of states around June, 2009, during which time the probability of low (high) frequency also became higher (lower). Switching features were also observed in September and December, 2009 and May, 2010. However, the high frequencies kept a short period of time. Finally, Panel D also shows that the jump probability was large from October, 2008 to June, 2009, which was consistent with the event of the financial crisis.

Mandelbrot (1963) and Fama (1965) report a volatility clustering feature in stock returns. This feature is also found in sport EUAs returns (Panel B of Figure 1). Volatility clustering (Cont, 2007) can be observed by the fact that the autocorrelation of squared spot EUAs returns is slowly decreasing. This is shown in Panel A of Figure 3.

**【Insert Figure 3】**

The estimated autocorrelation of squared spot EUAs returns under the RSJM reported in Panel B of Figure 3 indicates that the autocorrelation of squared spot EUAs returns is slowly decreasing. This evidence shows that the RSJM can capture the volatility clustering feature of spot EUAs returns in Phase I of the BlueNext. The above autocorrelation results also carry over to Phase II.

#### **4. Pricing futures and futures options on emission allowances**

In this section, the general Esscher transformation is introduced and applied to the RSJM to make it become a martingale process under two conditions. Whether

regime-switching risk is a source of systematic or unsystematic risk depends on the structure of filtration. In addition, a mean-reverting model is used to describe the process of convenience yields. Therefore, prices of futures and futures options are to be derived with a mean-reverting convenience yield model and the dynamics of spot EUAs is modeled by the RSJM under a no-arbitrage condition.

#### 4.1 *Two changes of measure in regime-switching jump diffusion*

Generally speaking, a unique martingale measure cannot be found when we consider asset returns with jump risks in an incomplete market. Gerber and Shiu (1994) used the Esscher transformation to price the options of insurance products in an incomplete market. The Esscher transformation has an advantage that the dynamic structure of invariance can be maintained after a measure transform. In addition, the existence condition of the moment generating function is still qualified regardless of the size of jump events. Furthermore, the Esscher transformation also can be regarded as the general Girsanov transformation. Based on a Markovian process of jump states, we promote a more flexible and general Esscher transformation with regime-switching jump risks.

Assume that a finite time is specified by  $[0, \mathcal{T}]$ , the filtration of spot EUAs price  $S(t)$  is denoted by  $\mathcal{F}_t^S$  and the filtration of a hidden Markov chain  $X$  is  $\mathcal{F}_t^X$ . Define the join filtrations of the EUAs and the hidden Markov chain as  $\sigma$ -algebras:  $\mathcal{G} = \sigma(\mathcal{F}_t^X \vee \mathcal{F}_t^S)$  and  $\mathcal{H} = \sigma(\mathcal{F}_T^X \vee \mathcal{F}_t^S)$ . Observing the filtrations  $\mathcal{G}$  and  $\mathcal{H}$ , we find that the filtration  $\mathcal{G}$  contains less information of the Markov chain than the filtration  $\mathcal{H}$ . The latter ( $\mathcal{H}$ ) provides investors the information regarding

the Markov-chain states risk. Then, the Esscher transform is defined by two different pricing kernels under the different filtrations. More specifically, the Esscher transform (Siu et al. 2008) is given as follows,

$$\left. \frac{d\mathbb{P}^h}{d\mathbb{P}} \right|_{\mathcal{M}} = E^P \left[ \frac{\exp\left(h^C \sigma W(T) + h^J \sum_{n=1}^{\Phi(T)} Z_n\right)}{E^P \left[ \exp\left(h^C \sigma W(T) + h^J \sum_{n=1}^{\Phi(T)} Z_n\right) \middle| \mathcal{F}_0^X \right]} \right] \Bigg|_{\mathcal{M}} \quad (9)$$

where  $h^C$  and  $h^J$  denote, respectively, the parameters of the Esscher transform associated with continuous and discontinuous motion, which is based on the Novikov's condition,  $E^P \left[ \exp\left(h^C \sigma W(T) + h^J \sum_{n=1}^{\Phi(T)} Z_n\right) \right] < \infty$ , and  $\mathcal{M} = \mathcal{G}$  or  $\mathcal{H}$ . In the Esscher transform framework, the risk induced by regime switching is priced (i.e., regime-switching risk or systematic risk) under the filtration  $\mathcal{G}$ , while it is not priced (i.e., unsystematic risk) under the filtration  $\mathcal{H}$ . This is because the filtration  $\mathcal{H}$  contains information  $\mathcal{F}_T^X$ , while the filtration  $\mathcal{G}$  does not contain sufficient information regarding regime-switching risk, and thereby being undiversifiable by an investment portfolio. We will elaborate more on it in the subsequent text.

(I) *The Case With Filtration  $\mathcal{H}$ : No Regime-Switching Risk Premium*

According to the definition of a martingale for the discounted stock price under the risk-neutral measure, the martingale condition can be shown as follows: (See **Appendix A**)

$$\mu + h^C \sigma^2 - r + \lambda_i (\phi(h^J + 1) - \phi(h^J)) = 0, \quad i = 1, 2 \quad \text{under } \mathcal{M} = \mathcal{H}$$

where  $\phi(h^J)$  denotes the moment generating function of the normal jump variable  $Z_n$  with mean  $\mu_J$  and variance  $\sigma_J^2$ . Because the asset returns with jumps are considered, Second Fundamental Theorem of asset pricing is not satisfied. Thus, there are infinite solutions for the Esscher-transform parameters that can satisfy the martingale condition (Also see Bo et al. 2010). The general Esscher transform is disassembled into continuous and discontinuous parts. We find a specific solution that satisfies the martingale condition as follows: (See **Appendix A**)

$$h_*^c = \frac{r - \mu}{\sigma^2}, \text{ and } h_*^J = \frac{-\mu_J - \frac{1}{2}\sigma_J^2}{\sigma_J^2}.$$

Based on the solution of the martingale condition under the filtration  $\mathcal{H}$ , the dynamic process of the spot EUAs by the Esscher transform under the risk-neutral measure  $\mathbb{Q}$  can be shown and given by: (See **Appendix A**),

$$\frac{dS(t)}{S(t-)} = rdt + \sigma dW^{\mathcal{Q}}(t) + d\left(\sum_{n=1}^{\Phi^{\mathcal{Q}}(t)} (e^{Z_n^{\mathcal{Q}}} - 1)\right) \quad (10)$$

where  $Z_n^{\mathcal{Q}}$  follows a normal distribution with mean  $-\frac{1}{2}\sigma_J^2$  and variance  $\sigma_J^2$ , and

$\Phi^{\mathcal{Q}}(t)$  denotes a new Markov-modulated Poisson process with a new intensity matrix given by

$$\Lambda^{\mathcal{Q}} = \begin{bmatrix} \lambda_1 \phi(h_*^J) & 0 \\ 0 & \lambda_2 \phi(h_*^J) \end{bmatrix} \quad (11)$$

where  $\phi(h_*^J) = E^P \left[ e^{h_*^J Z} \right] = \exp\left(-\frac{1}{2} \frac{\mu_J^2}{\sigma_J^2} + \frac{\sigma_J^2}{8}\right)$ .  $\lambda_i \phi(h_*^J)$  is the Markov-modulated

intensity (Bo et al. 2010). However, the invariant Markov chain  $X$  has an original matrix of the transition rates  $\Psi$  that remains unchanged under the risk-neutral measure. In addition, when  $\lambda_1$  is equal to  $\lambda_2$ , equation (10) will reduce to the JDM under the risk-neutral measure. Based on the new intensity matrix and the invariant Markov chain  $X$ , the joint probability under the risk-neutral measure is defined by

$$Q_{ij}(n, t) \equiv \mathbb{Q}(X(0) = i, X(t) = j, \Phi^\varrho(t) = n). \quad (12)$$

The joint probability under the risk-neutral measure can be determined from the moment generating function,  $\mathbf{P}(\xi, t) = \exp\left(\left(\Psi - (1 - \xi)\Lambda^\varrho\right)t\right)$ .

(II) *The Case With Filtration  $\mathcal{G}$ : Regime-Switching Risk Premium.*

By following Bo et al. (2010), the martingale condition can be shown to be: (See **Appendix A**)

$$\begin{aligned} \exp(-rt + \mu t - \frac{1}{2} \sigma^2 t) E^P \left[ \exp\left( (1 + h^C) \sigma W(t) + (1 + h^J) \sum_{n=1}^{\Phi(t)} Z_n \right) \middle| \mathcal{F}_0^X \right] \\ - E^P \left[ \exp\left( h^C \sigma W(t) + h^J \sum_{n=1}^{\Phi(t)} Z_n \right) \middle| \mathcal{F}_0^X \right] = 0 \end{aligned}$$

under  $\mathcal{M} = \mathcal{G}$ , where  $\mathcal{F}_0^X$  is given in a stationary state.

In the case of the filtration  $\mathcal{G}$ , a new Markov chain  $X^*$  has a new transition-rate matrix  $\Psi^*$  which is given in (13) by the first-order approximation of Taylor expansion:

$$\Psi^* = \begin{bmatrix} -\alpha_1^* & \alpha_1^* \\ \alpha_2^* & -\alpha_2^* \end{bmatrix} \approx \begin{bmatrix} -(\alpha_1 + (1 - \phi(h_*^J))\lambda_1) & (\alpha_1 + (1 - \phi(h_*^J))\lambda_1) \\ (\alpha_2 + (1 - \phi(h_*^J))\lambda_2) & -(\alpha_2 + (1 - \phi(h_*^J))\lambda_2) \end{bmatrix} \quad (13)$$

and  $(\pi_1^*, \pi_2^*) = \frac{1}{\alpha_1^* + \alpha_2^*} (\alpha_2^*, \alpha_1^*)$  denote new stationary sates. Therefore, with the new

intensity matrix and the new Markov chain, the new transition matrix under the risk-neutral measure is given by

$$Q_{ij}^*(n, t) \equiv \mathbb{Q}(X^\varrho(0) = i, X^\varrho(t) = j, \Phi^\varrho(t) = n) . \quad (14)$$

By observing the above result, the new joint probability  $Q_{ij}^*(n, t)$  is affected by the jump rate and the moment generating function of the jump variable. The terms  $(1 - \phi(h_*^J))\lambda_1$  and  $(1 - \phi(h_*^J))\lambda_2$  in  $\Psi^*$  are related to the premium of regime-switching risk for the following reason: if  $\phi(h_*^J)$  in (13) is equal to one, the new transition-rate matrix  $\Psi^*$  reduces to the original matrix  $\Psi$  in (6), and the new intensity matrix  $\Lambda^\varrho$  in (11) equals  $\Lambda$ . In this case, the risk premium terms disappear, and the transition-rate and the intensity matrices are unaltered by regime switching. Accordingly, regime switching is not a source of risk. However,  $\phi(h_*^J)$  would not be generally equal to 1. As such, regime switching causes changes in the transition-rate and the intensity matrices, and thereby inducing a source of risk which cannot be diversified. The associated risk premium is represented by the two extra terms in  $\Psi^*$  indicated above. This result can be further reasoned next.

The jump term in the pricing of futures options under the Merton's framework is regarded as unsystematic risk (Ballotta, 2005). Merton (1976) provides the equivalent martingale measure (or Merton measure) obtained by shifting the drift of a Brownian motion, but leaving the jump part unchanged by assuming that jump risk is

diversifiable (or unsystematic risk). Nevertheless, Jarrow and Rosenfeld (1984) provide empirical evidence showing that the jump component does affect the equilibrium prices of contingent claims, meaning that it is a source of systematic risk. Moreover, Ballotta (2005) finds that the Esscher measure appears to be the most suitable measure to capture the additional risk induced by the occurrence of crashes in the insurance market. Therefore, we consider the jump events occurred in the carbon market as a source of systematic risk. As such, investors require a risk premium for assuming the jump risk at each state, and hence the jump risk is priced. This fact has already been observed in the transition-rate matrix  $\Psi^*$  of the Markov-modulated Poisson process  $X^*$  after the Esscher transform is changed to the risk-neutral measure.

Finally, an empirical study is used to analyze the prices of futures options with regard to systematic and unsystematic risk via the different filtrations  $\mathcal{G}$  and  $\mathcal{H}$ . This is shown in the next section.

#### 4.2 Valuation of futures

##### (I) Constant Convenience Yield

We assume first a constant interest rate and a constant convenience yield. The futures price is determined by the following no-arbitrage condition:

$$F_c(t, T_1) = E^{\mathbb{Q}}[S(T_1) | \mathcal{F}_t] = S(t)e^{(r-\delta)(T_1-t)} \quad (15)$$

where  $F_c(t, T_1)$  denotes the daily futures price under a constant convenience yield  $\delta$ ,  $S(t)$  is the daily spot EUAs price,  $T_1$  is the futures contract maturity, and  $r$  is the

risk-free interest rate. Equation (15) with  $\delta = 0$  becomes a standard cost-of-carry model.

Daskalakis et al. (2009) adopt a JDM with a mean-reversion stochastic convenience yield to describe the relationship between the spot EUAs in Phase I and the EUA futures prices in Phase II. However, Uhrig-Homburg and Wagner (2009) disagree to use the stochastic convenience yield to examine the relation in Phase I and II. They find that in the case of EUA futures, intra-phase contracts (EUA futures commenced and expired in the same phase of the EU ETS) can be well described by the cost-of-carry model with zero convenience yields. Hence, we also investigate the contradictory issue of the convenience yield in intra-phase contracts.

We first estimate the convenience yield  $\delta(t_k)$  using the following equation:

$$\delta(t_k) = r - \frac{1}{T_1 - t} \ln \left( \frac{F(t_k, T_1)}{S(t_k)} \right) \quad (16)$$

where  $F(t_k, T_1)$  denotes the closing price of the EUA futures in ECX observed on day  $t_k$ , ( $t_k \leq T_1$  for every  $k$ ), and  $S(t_k)$  is the daily price of the spot EUAs. The convenience yield is estimated under the no-arbitrage condition. We then plot the time series of the estimated convenience yields from 26/02/2008 to 30/12/2010 in Figure 4. The evidence shows that the dynamics of the convenience yield is a mean-reverting process.

**【Insert Figure 4】**

*(II) Stochastic Convenience Yield*

Daskalakis et al. (2009) adopt a mean reverting random process under the risk-neutral measure to describe the behavior of the convenience yield given below:

$$d\delta_s(t) = [\kappa_s(\theta_s - \delta_s(t)) - \lambda_s\sigma_s]dt + \sigma_s dW_s(t) \quad (17)$$

where  $\kappa_s$  denotes the speed of mean-reversion,  $\theta_s$  represents a long-term mean yield,  $\sigma_s$  is the volatility of the convenience yield, and  $\lambda_s$  is the convenience-yield market price of risk. Then, the RSJM dynamics of spot EUAs prices with the stochastic convenience yield under the risk-neutral measure can be represented as follows:

$$\frac{dS(t)}{S(t-)} = (r - \delta(t))dt + \sigma dW^Q(t) + d\left(\sum_{n=1}^{\Phi^Q(t)} (e^{z_n^Q} - 1)\right). \quad (18)$$

Let  $\rho$  denote the instantaneous correlation between  $dW_s(t)$  and  $dW^Q(t)$  and the rest of the stochastic processes be mutually independent. Based on (17) and (18), the price of a futures contract with a stochastic convenience yield under the no-arbitrage condition can be solved and given by

$$F_s(t, T_1) = S(t)e^{r-H(t, T_1)\delta(t)} A(t, T_1) \quad (19)$$

where  $A(t, T_1) = \exp\left[\frac{[H(t, T_1) - (T_1 - t)](\kappa_s^2\theta_s - \kappa_s\lambda_s\sigma_s / 2 + \rho\sigma\sigma_s\kappa_s)}{\kappa_s^2} - \frac{\sigma_s^2 H^2(t, T_1)}{4\kappa_s}\right]$

and  $H(t, T_1) = \frac{1 - e^{-\kappa_s(T_1 - t)}}{\kappa_s}$  for all  $t \leq T_1$ .

Note that the futures prices given in (19) certainly involve the parameters of the mean reverting process of the convenience yield, and  $\sigma$  is the volatility of asset returns in (18) with jumps under the RSJM.

#### 4.3 Valuation of options on emission allowances

The Black's formula for pricing options on futures is well-known and given by

$$C_B(F_c) = C_B(F_c(t, T_1), K, r, T - t, \sigma) = e^{-r(T-t)} [F_c(t, T_1)N(d_1) - KN(d_2)] \quad (20)$$

where

$$d_1 = \frac{\ln \frac{F_c(t, T_1)}{K} + \frac{1}{2}(\sigma^2(T-t))}{\sqrt{\sigma^2(T-t)}}, \quad d_2 = d_1 - \sqrt{\sigma^2(T-t)},$$

$K$  = the strike price,  $T$  = the option's maturity,  $T \leq T_1$ .

The EUA futures price  $F_c(t, T_1)$  in (20) disregards the convenience yield ( $\delta = 0$ ) and  $\sigma$  is the volatility of asset returns without a jump ( $R_b$ ) defined in (2).

##### (I) Valuation of Options Under the JDM

For a given jump term ( $n > 0$ ) of the JDM, the price of a European call option on the EUA futures under the constant convenience yield is given by

$$\begin{aligned} C_J(F_c(t, T_1), K, r, T - t, \sigma, \sigma_J; n) &= e^{-r(T-t)} E_t^Q \left[ (F_c(T_1, T_1) - K)^+ \mid N^Q(t) = n \right] \\ &= e^{-r(T-t)} [F_c(t, T_1)N(d_1(n)) - KN(d_2(n))] \end{aligned} \quad (21)$$

where

$$d_1(n) = \frac{\ln \frac{F_c(t, T_1)}{K} + \frac{1}{2}(\sigma^2(T-t) + \sigma_J^2 n)}{\sqrt{\sigma^2(T-t) + \sigma_J^2 n}}, \quad d_2(n) = d_1(n) - \sqrt{\sigma^2(T-t) + \sigma_J^2 n},$$

$E_t^Q$  is a risk-neutral measure expectation at time  $t$ , and  $\sigma$  is the volatility of asset returns with jumps ( $R_j$ ) defined in (4). Equation (21) reduces to the Black's formula when the jump term ( $n$ ) is set zero. Hence, the pricing model of a European call option on the EUA futures under the JDM with a constant convenience yield is given by

$$C_J(F_c) \equiv \sum_{n=0}^{\infty} \left[ e^{-\lambda^*(T-t)} \frac{(\lambda^*(T-t))^n}{n!} C_J(F_c(t, T_1), K, r, T-t, \sigma, \sigma_j; n) \right] \quad (22)$$

where  $\lambda^* = \lambda\phi(h_*^J)$ . Note that equation (22) is a weighted sum of the Black's formulas subject to the  $n$ -th jump under a Poisson distribution.

## (II) Valuation of Options With Filtration $\mathcal{H}$ Under the RSJM

As observed in Section 4.1, the state of the Markov chain under the filtration  $\mathcal{H}$  is known to investors, and hence regime-switching risk is not priced. In addition,  $Q_{ij}(n, t)$  in (12) under  $\mathcal{H}$  has an invariant Markov chain and a new Poisson process with a new intensity matrix  $\Lambda^Q$ . Thus, under the filtration  $\mathcal{H}$  (without risk premium), the price of a European call option on the EUA futures with a constant convenience yield is given by

$$C_R(F_c(t, T_1), K, r, T-t, \sigma, \sigma_j; n) = e^{-r(T-t)} E_t^Q \left[ (F_c(T_1, T_1) - K)^+ \mid X(0) = i, X(t) = j, \Phi^Q(t) = n \right] \quad (23)$$

By observation, equation (23) is involved with not only the regime-switching probabilities, but also two jump risks of Poisson distributions. Thus, under the RSJM with a mean-reverting convenience yield model, the pricing model resembles a generalized Black's formula and can be easily derived as follows:

$$\begin{aligned}
C_R(F_s, Q) &= \sum_{n=0}^{\infty} \left[ \sum_{i,j \in \{1,2\}} \pi_i Q_{ij}(n, T-t) C_R(F_s(t, T_1), K, r, T-t, V(t, T, T_1), \sigma_j; n) \right] \\
&= \sum_{n=0}^{\infty} \left[ \sum_{i,j \in \{1,2\}} \pi_i Q_{ij}(n, T-t) \left( e^{-r(T-t)} [F_s(t, T_1) N(d_1(n)) - KN(d_2(n))] \right) \right] \quad (24)
\end{aligned}$$

where

$$d_1(n) = \frac{\ln \frac{F_s(t, T_1)}{K} + \frac{1}{2} (V(t, T, T_1)^2 + \sigma_j^2 n)}{\sqrt{V(t, T, T_1)^2 + \sigma_j^2 n}}, \quad d_2(n) = d_1(n) - \sqrt{V(t, T, T_1)^2 + \sigma_j^2 n}$$

$$\begin{aligned}
V(t, T, T_1)^2 &= \sigma^2 (T-t) \\
&+ \frac{\sigma_s^2}{\kappa_s} \left[ (T-t) - \frac{2}{k} (e^{-\kappa_s(T_1-T)} - e^{-\kappa_s(T_1-t)}) + \frac{1}{2\kappa_s} (e^{-2\kappa_s(T_1-T)} - e^{-2\kappa_s(T_1-t)}) \right] \\
&- \frac{2\rho\sigma_s\sigma}{\kappa_s} \left[ (T-t) - \frac{e^{-\kappa_s(T_1-T)} - e^{-\kappa_s(T_1-t)}}{\kappa_s} \right]
\end{aligned}$$

$$Q_{ij}(n, t) \equiv \mathbb{Q}(X(0) = i, X(t) = j, \Phi^Q(t) = n).$$

Moreover, the EUA futures price  $F_s(t, T_1)$  in (24) is defined in (19) with a stochastic convenience yield and the volatility  $\sigma$  is the spot return ( $R_R$ ) volatility given in (7) under the RSJM. In addition, the volatility  $V(t, T, T_1)$  of the futures return is composed of the volatility of  $R_R$  and the parameters of the mean-reverting convenience yield model. When the stochastic convenience-yield model is disregarded,  $V(t, T, T_1)^2$  reduces to  $\sigma^2(T-t)$  and the call option  $C_R(F_s, Q)$  in (24) becomes the pricing model of a futures call option under the RSJM with a constant convenient yield, called it  $C_R(F_c, Q)$ . In addition, the joint probability  $Q_{ij}(n, T-t)$ , and the Markov-chain transition rate in (24) are unchanged under the risk-neutral measure, implying that the Markov chain uncertainty induces a source of unsystematic risk under the filtration  $\mathcal{H}$ .

(III) *Valuation of Options With Filtration  $\mathcal{G}$  Under the RSJM*

Next, we consider the case where the Markov chain uncertainty induces a source of systematic risk. When the filtration is conditional on  $\mathcal{G} (= \mathcal{M})$  in the Esscher transform as shown in (9), the regime switching via the Markov chain induces regime-switching risk, a source of system risk, that is priced in the option valuation. As mentioned earlier, the transition-rate matrix under the risk-neutral measure  $\mathbb{Q}$  is changed to  $\Psi^*$  which implies the existence of risk premiums  $(1 - \phi(h_*^j))\lambda_i$  given in (13). Thus, with regard to regime-switching risk, the pricing model of a futures call option under the RSJM is given by (25) below:

$$C_R(F_s, Q^*) = \sum_{n=0}^{\infty} \left[ \sum_{i,j \in \{1,2\}} \pi_i^* Q_{ij}^*(n, T-t) C_R(F_s(t, T_1), K, r, T-t, V(t, T, T_1), \sigma_j, n) \right] \quad (25)$$

where  $Q_{ij}^*(n, t) \equiv \mathbb{Q}(X^Q(0) = i, X^Q(t) = j, \Phi^Q(t) = n)$  with the new transition rate matrix  $\Psi^*$  and new  $(\pi_1^*, \pi_2^*)$  defined in (13).

*Proof: Appendix B*

In the same way, the pricing model (25) becomes  $C_R(F_c, Q^*)$  under the RSJM with a constant convenience yield when Markov-chain risk is priced. Finally, we note that both the pricing models (24) and (25) for the environmental carbon market are of a weighted sum (or portfolio) of the Black's formulas under the RSJM with Markov-chain probabilities as the weights.

## 5. Empirical analysis of emission allowances market.

The root mean squared error (RMSE) is employed as a criterion to estimate the parameters of the mean-reverting convenience yield model. The RMSE is given in (26)

below:

$$\sqrt{\frac{1}{m_{\mathbf{D}}} \sum_{k=1}^{m_{\mathbf{D}}} \left( \frac{F_{\mathbf{M}}(t_k) - F_{\mathbf{D}}(t_k)}{F_{\mathbf{D}}(t_k)} \right)^2} \quad (26)$$

where  $F_{\mathbf{M}}(t_k)$  is the theoretical price at time  $t_k$ ,  $F_{\mathbf{D}}(t_k)$  is the daily futures closing prices of EUAs on ECX at time  $t_k$ , and  $m_{\mathbf{D}}$  is the total number of observations. The pricing performance of the derived formulas is next analyzed, respectively, for out-the-money (OTM), at-the-money (ATM), and in-the-money (ITM) futures options with the RMSE criterion.

### 5.1 Empirical Analysis: Futures of Emission Allowances

The ECX data are collected daily for EUA futures from 01/11/2010 to 30/12/2010. The futures are Mar-11, Jun-11, Sep-11, and Dec-11 contracts of year 2011. Let  $\lambda_s$  be zero as used in Daskalakis et al. (2009).<sup>3</sup> The parameters  $(\kappa_s, \theta_s, \sigma_s, \rho)$  of the mean-reverting convenience yield model are estimated via the minimal RMSE criterion on the convenience yield series and the resulting estimates are reported in Table 4. The RMSE for Mar-11, Jun-11, Sep-11, and Dec-11 contracts are, respectively,  $1.1435 \cdot 10^{-4}$ ,  $1.2414 \cdot 10^{-4}$ ,  $1.2560 \cdot 10^{-4}$ ,  $3520 \cdot 10^{-4}$ . The estimated parameters are very small about  $10^{-4}$  in intra-phase II (EUA futures commenced and expired in Phase II), which is similar to Daskalakis et al. (2009) and Uhrig-Homburg et al. (2009). They also provide evidence to show a zero stochastic convenience yield in futures prices in intra-phase I.

---

<sup>3</sup> Daskalakis et al. assume that  $\lambda_s$  and  $\rho$  are zeros.

【Insert Table 4】

## 5.2 Empirical Analysis of Futures Options on Emission Allowances

Abate and Whitt (1992) provide a numerical method of generating the probability matrix  $Q(n,t)$  and  $Q^*(n,t)$  that are, respectively, used in (12) and (14).

The riskless rate of interest rate  $r$  is the average annual Euribor in year 2010 which is 1.3407%. The observed call option data contain Mar-11, Jun-11, Sep-11, Dec-11 futures options at ECX with strike prices 12,12.5,13,13.5,14,14.5,15, and 15.5. There are 256 trading days per year.

To test the derived pricing models, the observations are divided into in- and out-sample groups. The in-sample period starts from 01/11/2010 to 30/12/2010 and the out-sample period is from 03/01/2010 to 28/02/2011. The OTM, ATM and ITM options are those options, respectively, with  $S/K < 0.95$ ,  $0.95 \leq S/K \leq 1.05$ , and  $S/K > 1.05$ . The pricing errors of the futures options are reported for the six pricing models such as  $C_B(F_c)$ ,  $C_J(F_c)$ ,  $C_R(F_c, Q)$ ,  $C_R(F_s, Q)$ ,  $C_R(F_c, Q^*)$ , and  $C_R(F_s, Q^*)$ . The total pricing errors of the OTM, AMT, and IMT futures options reported in Table 5 for the in-sample period are 0.0992 under  $C_B(F_c)$ , 0.0832 under  $C_J(F_c)$ , 0.0765 under  $C_R(F_c, Q)$ , 0.1124 under  $C_R(F_s, Q)$ , 0.0566 under  $C_R(F_c, Q^*)$ , and 0.0515 under  $C_R(F_s, Q^*)$ . In the out-sample period case, the total pricing errors of the futures options are 0.1640 under the  $C_B(F_c)$ , 0.1488 under  $C_J(F_c)$ , 0.1430 under  $C_R(F_c, Q)$ , 0.1928 under  $C_R(F_s, Q)$ , 0.1190 under  $C_R(F_c, Q^*)$ , and 0.1112 under  $C_R(F_s, Q^*)$ . By combining all of the options in the dataset, the total pricing errors of the futures

options are 0.1354 under  $C_B(F_c)$ , 0.1204 under  $C_J(F_c)$ , 0.1146 under  $C_R(F_c, Q)$ , 0.1574 under  $C_R(F_s, Q)$ , 0.0924 under  $C_R(F_c, Q^*)$ , and 0.0854 under  $C_R(F_s, Q^*)$ .

**【Insert Table 5】**

We observe the above results that all models perform better in the in-sample period than in the out-sample period. In all cases, the pricing errors of the OTM options are larger than those of the ITM options. In the model testing for the different time periods, we find that the JDM performs better than the BSM model under a zero convenience yield, i.e., the  $C_J(F_c)$  has a RMSE less than the  $C_B(F_c)$ , regardless of the in- or out-sample period, which is consistent with Daskalakis et al. (2009) showing that the carbon market exhibits a jump feature at different Phases. With regard to regime switching risk premium, the derived futures option pricing model [ $C_R(F_s, Q^*)$ ] under the RSJM with a stochastic convenience yield has the lowest total RMSE among all other models in the in- and out- sample periods as well as in the whole period. That is, the  $C_R(F_s, Q^*)$  is the best performer. In addition, the  $C_R(F_s, Q^*)$  has a lower RMSE than the  $C_R(F_s, Q)$  with a zero convenience yield. And also, the  $C_R(F_c, Q^*)$  shows a lower total RMSE than the  $C_R(F_c, Q)$  under the two pricing kernels. These results clearly indicate that Markov-chain risk is a priced systematic risk and should be incorporated into the valuation of futures options in the carbon market. This conclusion is also supported by Siu et al. (2009) who show using numerical experiments that regime-switching risk has a significant impact on the pricing of options.

Adding a stochastic convenience yield does not improve the accuracy of the

pricing of futures options. Specifically, the total RMSE of the  $C_R(F_s, Q^*)$  is slightly smaller than (or about the same as) that of the  $C_R(F_c, Q^*)$  in all the test periods. However, the  $C_R(F_s, Q)$  performs marginally worse than the  $C_R(F_c, Q)$  in terms of the RMSE.<sup>4</sup> Thus, using a stochastic convenience yield adds not much to improve the pricing accuracy.

In summary, the derived futures option pricing models are empirically tested using the ECX data, and the six theoretical call option models,  $C_B(F_c)$ ,  $C_J(F_c)$ ,  $C_R(F_c, Q)$ ,  $C_R(F_s, Q)$ ,  $C_R(F_c, Q^*)$ , and  $C_R(F_s, Q^*)$  are empirically compared for their pricing accuracy in terms of the size of RMSE. In All cases, the theoretical pricing model of futures options derived under the RSJM with a stochastic convenience yield is the best performer, when the regime-switching risk premium is considered in the pricing of options. Its RSJM counterpart with a constant convenience yield has almost the same good performance.

## 6. Conclusion

We examine the spot EUAs return in the BlueNext that exhibits a volatility clustering feature and show that the carbon-market system is impacted by announcements of CO<sub>2</sub> emissions policies. We test empirically the dynamic processes such as the BSM (or GMP), the JDM, and the RSJM to check which model can provide a better fit to the spot EUAs return of the BlueNext in France. Though the JDM performs better than the BSM, the RSJM has the highest explanatory power among all the models considered for the carbon allowance market.

---

<sup>4</sup> This result carries over to the pricing models of the futures options derived from the JDM with a constant and a stochastic convenience yield.

Moreover, the theoretical pricing models of futures options are derived based on the BSM, the JDM and the RSJM. The RSJM pricing models with a constant and a stochastic convenience yield are obtained via a generalized Esscher transform that leads to two types of filtration, one of them associated with a risk premium in the carbon-market environment. When regime-switching risk is incorporated, the derived pricing models of futures options under the RSJM with a stochastic convenience yield exhibit the best empirical performance. Due to the fact that carbon markets are frequently impacted by changes in CO<sub>2</sub> emissions policies, the regime-switching risk induced by Markov-chain uncertainty is an important pricing factor that should be incorporated in the valuation of futures options. In addition, using a stochastic convenience yield improves slightly the pricing accuracy under the RSJM, but not under the JDM.

In summary, a good pricing model should be able to capture the macroeconomic impacts of good or bad news and to transmit properly the impacts into the model dynamics of spot EUAs. Thus, the RSJM is concluded to be the best model to fit the price behavior of the carbon market in EU ETS and to price its related derivatives.

## Appendix A

We consider a martingale condition by showing that the expectation  $E^Q \left[ S(t) | \sigma(\mathcal{F}_0^S \vee \mathcal{F}_T^X) \right]$  is equal to the initial price  $S(0)$  under the risk-neutral measure  $\mathbb{Q}$ .

$$E^P \left[ S(0) e^{-rt + \mu t - \frac{1}{2} \sigma^2 t + \sigma W(t) + \sum_{n=1}^{\Phi(t)} Z_n} \frac{e^{h^C \sigma W(t)}}{E^P \left[ e^{h^C \sigma W(t)} | \mathcal{F}_0^S \right]} \frac{e^{h^J \sum_{n=1}^{\Phi(t)} Z_n}}{E^P \left[ e^{h^J \sum_{n=1}^{\Phi(t)} Z_n} | \mathcal{F}_0^X \right]} \middle| \sigma(\mathcal{F}_0^S \vee \mathcal{F}_T^X) \right] = S(0) \quad (\text{A1})$$

where  $\frac{d\mathbb{P}^h}{d\mathbb{P}} \bigg|_{\sigma(\mathcal{F}_0^S \vee \mathcal{F}_T^X)} = \frac{e^{h^C \sigma W(t)}}{E^P \left[ e^{h^C \sigma W(t)} | \mathcal{F}_0^S \right]} \frac{e^{h^J \sum_{n=1}^{\Phi(t)} Z_n}}{E^P \left[ e^{h^J \sum_{n=1}^{\Phi(t)} Z_n} | \mathcal{F}_0^X \right]}$  is a pricing kernel of the

Esscher transform under  $\sigma(\mathcal{F}_0^S \vee \mathcal{F}_T^X)$ . We divide the RSJM into two parts: a continuous dynamic process and a jump dynamic process. Therefore, the martingale condition (A1) can be simplified as the following equation:

$$\mu + h^C \sigma^2 - r + \lambda_i (\phi(h^J + 1) - \phi(h^J)) = 0, \quad i = 1, 2$$

and it can be satisfied with  $h_*^C = \frac{r - \mu}{\sigma^2}$  and  $h_*^J = \frac{-\mu_J - \frac{1}{2} \sigma_J^2}{\sigma_J^2}$ .

Since the continuous and the jump dynamic processes are independent of each other,  $\{W(t)\} \perp \left\{ \sum_{n=1}^{\Phi(t)} Z_n \right\}$ , we apply, respectively, the Esscher transform to the continuous party  $\{W(t)\}$  and the jump party  $\left\{ \sum_{n=1}^{\Phi(t)} Z_n \right\}$ . The result of the continuous

party is similar to Girsanov theorem. Thus, the new standard Brownian motion  $W^*(t)$  under  $\mathbb{P}^h$  is given by  $dW^*(t) = dW(t) - \sigma h^C dt$ , where the asterisk  $*$  means the new process with the new parameter under the changed measure. The size of jump  $\{Z_n^*\}$  has a new probability density  $N(\mu_J^*, \sigma_J^{*2})$  with  $\mu_J^* = \mu_J + h^J \sigma_J^2$ , and  $\sigma_J^* = \sigma_J$ .

By using equation (9) under the risk-neutral measure  $\mathbb{Q}$  with  $\mathcal{G}_0 (= \sigma(\mathcal{F}_0^S \vee \mathcal{F}_0^X))$ , we have

$$E^P \left[ S(0) e^{-rt + \mu t - \frac{1}{2} \sigma^2 t + \sigma W(t) + \sum_{n=1}^{\Phi(t)} Z_n} \frac{e^{h^C \sigma W(t)}}{E^P \left[ e^{h^C \sigma W(t)} \middle| \mathcal{F}_0^S \right]} \frac{e^{h^J \sum_{n=1}^{\Phi(t)} Z_n}}{E^P \left[ e^{h^J \sum_{n=1}^{\Phi(t)} Z_n} \middle| \mathcal{F}_0^X \right]} \middle| \mathcal{G}_0 \right] = S(0) \quad (\text{A2})$$

where  $\frac{d\mathbb{P}^h}{d\mathbb{P}} \Big|_{\mathcal{G}_0} = \frac{e^{h^C \sigma W(t)}}{E^P \left[ e^{h^C \sigma W(t)} \middle| \mathcal{F}_0^S \right]} \frac{e^{h^J \sum_{n=1}^{\Phi(t)} Z_n}}{E^P \left[ e^{h^J \sum_{n=1}^{\Phi(t)} Z_n} \middle| \mathcal{F}_0^X \right]}$  is a pricing kernel of the

Esscher transform under  $\mathcal{G}_0$ . We also divide the RSJM into two parts: continuous and jump dynamic processes. Therefore, the martingale condition (A2) leads to the following equation

$$-rt + \mu t - \frac{1}{2} \sigma^2 t + \frac{1}{2} \left[ (h^C + 1) \sigma \right]^2 t - \frac{1}{2} (h^C \sigma)^2 t = 0, \text{ and } E^P \left[ \frac{e^{(1+h^J) \sum_{n=1}^{\Phi(t)} Z_n}}{E^P \left[ e^{h^J \sum_{n=1}^{\Phi(t)} Z_n} \middle| \mathcal{F}_0^X \right]} \middle| \mathcal{G}_0 \right] = e^0 = 1$$

which can be satisfied with  $h_*^C = \frac{r - \mu}{\sigma^2}$  and  $h_*^J = \frac{-\mu_J - \frac{1}{2} \sigma_J^2}{\sigma_J^2}$ .

Next, we consider the following equations after a change of measure under  $\mathcal{G}_0$

$$\frac{\mathbb{P}^{h^j} \left( Z_1^* \in dz_1, Z_2^* \in dz_2, \dots, Z_m^* \in dz_m, \Phi^*(t) = m, X^*(0) = i, X^*(t) = j \right)}{\mathbb{P} \left( Z_1 \in dz_1, Z_2 \in dz_2, \dots, Z_m \in dz_m, \Phi(t) = m, X(0) = i, X(t) = j \right)} = \frac{e^{h^j \sum_{n=1}^m Z_n}}{E^P \left[ e^{h^j \sum_{n=1}^m Z_n} \middle| \mathcal{F}_0^X \right]}$$

$$\mathbb{P} \left( Z_1^* \in dz_1, Z_2^* \in dz_2, \dots, Z_m^* \in dz_m, \Phi^*(t) = m, X^*(0) = i, X^*(t) = j \right)$$

$$= \frac{e^{h^j \sum_{n=1}^m Z_n}}{E^P \left[ e^{h^j \sum_{n=1}^m Z_n} \middle| \mathcal{F}_0^X \right]} \mathbb{P}(Z_1^* \in dz_1) \cdot \mathbb{P}(Z_2^* \in dz_2) \cdots \mathbb{P}(Z_m^* \in dz_m) \mathbb{P}(\Phi^*(t) = m, X^*(0) = i, X^*(t) = j)$$

$$= \frac{e^{h^j z_1}}{\phi(h^j)} f_{Z_1}(z_1) \cdot \frac{e^{h^j z_2}}{\phi(h^j)} f_{Z_2}(z_2) \cdots \frac{e^{h^j z_m}}{\phi(h^j)} f_{Z_m}(z_m) \frac{\phi(h^j)^m}{E^P \left[ e^{h^j \sum_{n=1}^m Z_n} \middle| \mathcal{F}_0^X \right]} P(m, t).$$

Let  $f_Z^*$  be  $\frac{e^{h^j z}}{\phi(h^j)} f_Z(z)$  and  $Q(m, t; h^j)$  be  $\frac{\phi(h^j)^m}{E^P \left[ e^{h^j \sum_{n=1}^m Z_n} \middle| \mathcal{F}_0^X \right]} P(m, t)$ . Hence, we have

the new probability density function of  $f_Z^*$  and the new Markov chain  $Q(m, t; h^j)$ .

Finally, we have

$$\exp(\Psi^* t) \approx \exp \left[ \Psi - (1 - \phi(h_*^j)) \Lambda \right] t$$

By using the first-order approximation of Taylor expansion, we have

$$\Psi^* = \begin{bmatrix} -\alpha_1^* & \alpha_1^* \\ \alpha_2^* & -\alpha_2^* \end{bmatrix} = \begin{bmatrix} -(\alpha_1 + (1 - \phi(h_*^j))\lambda_1) & (\alpha_1 + (1 - \phi(h_*^j))\lambda_1) \\ (\alpha_2 + (1 - \phi(h_*^j))\lambda_2) & -(\alpha_2 + (1 - \phi(h_*^j))\lambda_2) \end{bmatrix}$$

with the new transition rate and  $(\pi_1^*, \pi_2^*) = \frac{1}{\alpha_1^* + \alpha_2^*} (\alpha_2^*, \alpha_1^*)$ .

## Appendix B

Consider a European call option

$$\begin{aligned}
E^{P^{h_*}} \left[ e^{-rt} (F_M(t) - K)^+ \middle| \mathcal{F}_T^X \right] &= e^{-rt} E^P \left[ F_M(0) e^{ut - \frac{1}{2}\sigma_t^2 - \eta(t) + \langle \mathbf{1}, \mathcal{Y}_t \rangle} \frac{e^{\langle \mathbf{h}_*, \mathcal{Y}_t \rangle}}{E^P \left[ e^{\langle \mathbf{h}_*, \mathcal{Y}_t \rangle} \middle| \sigma(\mathcal{F}_0^S \vee \mathcal{F}_0^X) \right]} \mathbf{1}_{\{S(t) \geq K\}} \middle| \mathcal{F}_T^X \right] \\
&\quad - e^{-rt} K \mathbb{P}^{h_*} \left[ F_s(t) \geq K \middle| \mathcal{F}_T^X \right] \\
&= F_M(0) \sum_{n=0}^{\infty} \sum_{ij=1}^I N(d_1(n)) \pi_i Q_{ij}(n, t) - e^{-rt} \sum_{n=0}^{\infty} \sum_{ij=1}^I N(d_1(n)) \pi_i Q_{ij}(n, t)
\end{aligned}$$

where  $\mathcal{Y}_t = \left( \sigma W(t), \sum_{n=1}^{\Phi(t)} Z_n \right)$ ,  $\mathbf{h}_* = (h_*^C, h_*^J)$ ,  $\langle \cdot, \cdot \rangle$  is an inner product, and  $M = s$

or  $c$ .

We simplify the above result to give Equation (24). That is

$$CF_R(F_M(t, T_1), K, r, T-t, V(t, T, T_1), \mathcal{Q}) = \sum_{n=0}^{\infty} \left[ \sum_{i,j \in I} \pi_i Q_{ij}(n, \tau; h_*^J) CF(F_M(t, T_1), K, r, T-t, V(t, T, T_1), \sigma_j, n) \right].$$

Equation (25) can be derived in a similar way.

## **BIBLIOGRAPHY**

- Abate, J., and Whitt, W., (1992). Numerical inversion of probability generating functions. *Operations Research Letters* 12, 245-251.
- Alberola, E., Chevallier, J., (2009). European carbon prices and banking restrictions: evidence from phase I (2005-2007). *The Energy Journal* 30, 51-80.
- Alberola, E., Chevallier, J., and Chéze, B., (2008). Price drivers and structural breaks in European carbon price 2005-2007. *Energy Policy* 36, 787-797.
- Ballotta, L., (2005). A Lévy process-based framework for the fair valuation of participating life insurance contracts. *Insurance: Mathematics and Economics* 37, 173-196.
- Benz, E., and Trück, S., (2009). Modeling the price dynamics of CO<sub>2</sub> emission allowances. *Energy Economics* 31, 4-15.
- Black, F., and Scholes, M., (1973). The pricing of options and corporate liabilities. *The Journal of Political Economy* 81, 3, 637-654.
- Bo, L., Wang, Y., and Yang, X., (2010). Markov-modulated jump-diffusions for currency option pricing. *Insurance: Mathematics and Economics* 46, 461-469.
- Borovkov, K., Decrouez, G., and Hinz, J., (2010). Jump-diffusion modeling in emission markets. *Stochastic Models* 27, 50-76.
- Bunn, D., Fezzi, C., (2007). Interaction of European carbon trading and energy prices. *Fondazione Eni Enrico Mattei Working Paper* 123
- Carmona, R., Fehr, F., and Hinz, J., (2009). Optimal stochastic control and carbon price formation. *SIAM. Journal of Control and Optimization* 48, 2168-2190.
- Cetin, U., and Verschuere, M., (2010). Pricing and hedging in carbon emissions markets. *International Journal of Theoretical and Applied Finance* 12, 949-967.
- Chevalier, J., (2009). Carbon futures and macroeconomic risk factors: a view from the EU ETS. *Energy Economics* 31. 614-625.
- Christiansen, A., Arvanitakis, A., Tangen, K., and Hasselknippe, H., (2005). Price determinants in the EU emissions trading scheme. *Climate Policy* 5, 15-30.
- Cont, R., (2007). Volatility clustering in financial markets: empirical facts and agent-based models. *Long Memory in Economics*, 289-310.
- Convery, F.J., Redmond, L., (2007). Market and piece developments in the European Union Emissions Trading Scheme. *Review of Environmental Economics and*

Policy 1, 88-111.

- Daskalakis, G., Psychoyios, D., and Markellos., R. N., (2009). Modeling CO<sub>2</sub> emission allowance prices and derivatives: evidence from the European trading scheme. *Journal of Banking and Finance* 33, 1230-1241.
- Dempster, A.P., Larid, N.M., and Rubin, D.B., (1977). Maximum likelihood from incomplete data via the EM algorithm. *Journal of the Royal Statistical Society. Series B* 39, 1-38.
- Denny, A. E. Convery, F. J., and De Perthuis, C., (2010). Pricing carbon: the European Union Emissions Trading Scheme. Printed in the United Kingdom at the University Press, Cambridge.
- Fama, E.F., (1965). The Behavior of stock-market prices. *The Journal of Business* 38, 34-105.
- Gerber, H.U., and Shiu E.S.W., (1994). Option pricing by Escher transforms. *Transactions of Society of Actuaries* 46, 99-140.
- Hilliard, J. E., and Reis, J., (1998). Valuation of commodity futures and options under stochastic convenience yields, interest rates, and jump diffusions in the spot. *Journal of Financial and Quantitative Analysis* 33, 61-86.
- Hinz, J., and Novikov, A., (2010). On fair pricing of emission-related derivatives. *Bernoulli* 16, 1240-1261.
- Jarrow, R.A. and Rosenfeld, E. (1984). Jump risks and the intertemporal capital asset pricing model. *Journal of Business* 57, 337-351
- Kanen, J.L.M., (2006). Carbon trading and pricing. *Environmental Finance Publications*.
- Kou, S.G., (2002). A Jump-diffusion model for option pricing. *Management Science* 8, 1086-1101.
- Lange, K. A, (1995). Gradient algorithm locally equivalent to the EM algorithm. *Journal of the Royal Statistical Society. Series B (Methodological)* 57, 425-437.
- Last, G., and Brandt, A., (1995). *Marked Point Processes on the Real Line: The Dynamic Approach*. Springer.
- Mandelbrot, B., (1963). The variation of certain speculative prices. *The Journal of Business* 36, 394-419.
- Mansanet-Bataller, M., Pardo, A., and Valor, E., (2007). CO<sub>2</sub> price, energy and weather. *The Energy Journal* 28, 73-92.

- Meng, X.L. and Rubin, D.B., (1991). Using EM to obtain asymptotic variance-covariance: the SEM algorithm. *Journal of the American Statistical Association* 86, 899-909.
- Merton, R. C., (1976). Option pricing when underlying stock returns are discontinuous. *Journal of Financial Economics* 3, 125-144.
- Seifert, J., Uhrig-Homburg, M., and Wanger, M., (2008). Dynamic behavior of CO<sub>2</sub> spot prices. *Journal of Economics and Management* 56, 180-194.
- Siu, T. K., and Yang, H., (2008). Option pricing when the regime-switching risk is priced. *Acta Mathematicae Applicatae Sinica, English Series* 25, 369-388.
- Uhrig-Homburg, M., and Wagner, M., (2009). Futures price dynamics of CO<sub>2</sub> emission allowances: an empirical analysis of the trial period. *Journal of Derivatives* 17, 73-88.

**Table 1:** The Evolution of The Trading Value in the Carbon Market From 2005 to 2010

The carbon trading markets are divided into two categories of carbon products; one is the carbon emission trading system including European Union Emissions Trading (EU ETS), the New South Wales (NSW), the Chicago Climate Exchange (CCE), the Regional Greenhouse Gas Initiative (RGGI), and the Assigned Amount Units (AAU). The other is the greenhouse gas reduction projects in Kyoto Protocol, including the Clear Development Mechanism (CDM), and the Joint Implementation and the voluntary market. Table 1 represents the evolution of the trading value in the carbon markets from 2005 to 2010. The other allowances involve the trading carbon value in NSW, CCE, RGGI, and AAU, and the other offset covers the Joint Implementation and the voluntary market. The trading value of EUAs increased from 2005 to 2010, and EUAs accounts for 84 percent of global carbon market value in 2010. Data source comes from state and trends of the carbon market in carbon finance by the World Bank in 2011.

Value (\$Billion)	EU ETS Allowances	Other Allowances	Primary CDM	Secondary CDM	Other Offsets	Total
2005	7.9	0.1	2.6	0.2	0.3	11.0
2006	24.4	0.3	5.8	0.4	0.3	31.2
2007	49.1	0.3	7.4	5.5	0.8	63.0
2008	100.5	1.0	6.6	26.3	0.8	135.1
2009	118.5	4.3	2.7	17.5	10.7	143.7
2010	119.8	1.1	1.5	18.3	1.2	141.9

**Table 2:** Statistics of the Spot EUAs Returns in BlueNext

<b>BlueNext</b>	Phase I		Phase II
	Period I	Period II	Period III
Number of Obs.	216	412	742
Maximum	0.0854	0.5108	0.1055
Minimum	-0.1343	-0.5108	-0.1029
Mean	0.0011	-0.0163	-0.0006
Variance	0.0006	0.0086	0.0006
Skewness	-1.0244	-0.1525	-0.2680
Kurtosis	8.7496	9.2656	5.2771
Number of returns more than 5%	5 (0.0643)	51 (0.1328)	9 (0.0723)
Number of returns less than -5%	6 (-0.0848)	96 (-0.1336)	25 (-0.0662)
Total	11	147	34

- Note: 1. The spot EUAs prices in BlueNext started from 24/06/ 2005 to 30/12/2010.  
2. The parentheses denote the mean of returns more than 5% or less than -5%.  
3. The results of EEX are similar, so omitted it.

**Table 3:** Estimated Parameters of the BSM, the JDM and the RSJM in the Spot Market at BlueNext

Time	Model	$p_{11}$	$p_{22}$	$\bar{\mu}$	$\mu_J$	$\sigma$	$\sigma_J$	$\lambda_1$	$\lambda_2$	LRT
Period I	BSM	--	--	0.0011	--	0.0251	--	--	--	
24/06/2005		--	--	(0.0017)	--	(0.0012)	--	--	--	
24/04/2006	JDM	--	--	0.0024	-0.0026	0.0112	0.0314	0.4846	--	61.89*
		--	--	(0.0013)	(0.0038)	(0.0013)	(0.0018)	(0.3939)	--	
Period II	BSM	--	--	-0.0163	--	0.0924	--	--	--	
01/06/2006		--	--	(0.0046)	--	(0.0032)	--	--	--	
28/12/2007	JDM	--	--	0.0004	-0.0171	0.0074	0.0879	0.9789	--	328.89*
		--	--	(0.0008)	(0.0046)	(0.0003)	(0.0019)	(0.4902)	--	
Phase I	BSM	--	--	-0.0108	--	0.0805	--	--	--	
24/06/2005		--	--	(0.0031)	--	(0.0022)	--	--	--	
28/12/2007	JDM	--	--	0.0005	-0.0180	0.0114	0.0947	0.6279	--	632.38*
		--	--	(0.0004)	(0.0051)	(0.0004)	(0.0014)	(0.1377)	--	
	RSJM	0.9868	0.9830	0.0005	-0.0190	0.0168	0.0982	0.0009	1.0460	134.21*
		(0.0068)	(0.0087)	(0.0009)	(0.0052)	(0.0008)	(0.0065)	(0.0068)	(0.1022)	
Phase II	BSM	--	--	-0.0006	--	0.0239	--	--	--	
26/02/2008		--	--	(0.0009)	--	(0.0006)	--	--	--	
30/12/2010	JDM	--	--	0.0016	-0.0073	0.0169	0.0302	0.2974	--	67.75*
		--	--	(0.0010)	(0.0060)	(0.0032)	(0.0034)	(0.3201)	--	
	RSJM	0.9852	0.9773	0.0014	-0.0028	0.0158	0.0210	0.0003	1.7970	79.89*
		(0.0071)	(0.0113)	(0.0008)	(0.0014)	(0.0007)	(0.0028)	(0.0058)	(0.4195)	

Note: 1. (•) denotes the standard deviation estimated by the SEM algorithm.

2. JDM represents the jump diffusion model, and RSJM is the regime switching jump diffusion model.

3. LRT represents the likelihood ratio test between the null hypothesis of the jump diffusion model and the alternative hypothesis of the regime switching jump diffusion model.

4. The parameters in EEX are also estimated, but the trading volume in EEX is thinner than BlueNext, and so omitted it.

**Table 4:** The Parametric Estimation of The Stochastic Convenience Yield

Parameters of convenience yield*10 <sup>-4</sup>	Mar-11	Jun-11	Sep-11	Dec-11
$\kappa_s$	0.1280	0.1366	0.1343	0.1344
$\theta_s$	0.1163	0.1130	0.1182	0.1173
$\sigma_s$	0.0295	0.0260	0.0253	0.0235
$\rho$	0.1218	0.1241	0.1230	0.1240
RMSE	1.1435	1.2414	1.2560	1.3520

Note:1. The parameters ( $\kappa_s, \theta_s, \sigma_s, \rho$ ) are calculated through Equation (19) for the period from 09/04/2008 to 30/12/2010 in ECX.

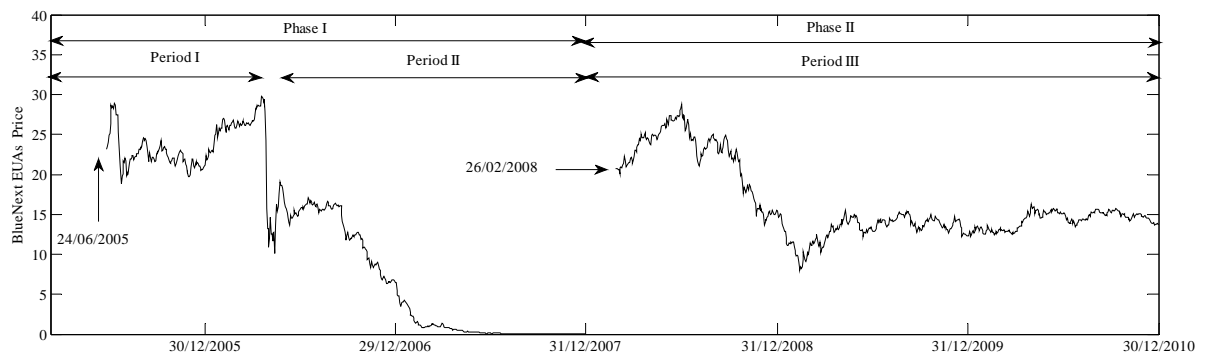
2. RMSE refers to the relative mean square error, which is expressed in 10<sup>-4</sup>.

**Table 5:** The Futures Option Pricing Errors measured by RMSE With The Underling for ECX with Mar-11, Jun-11, Sep-11and Dec-11 futures contracts.

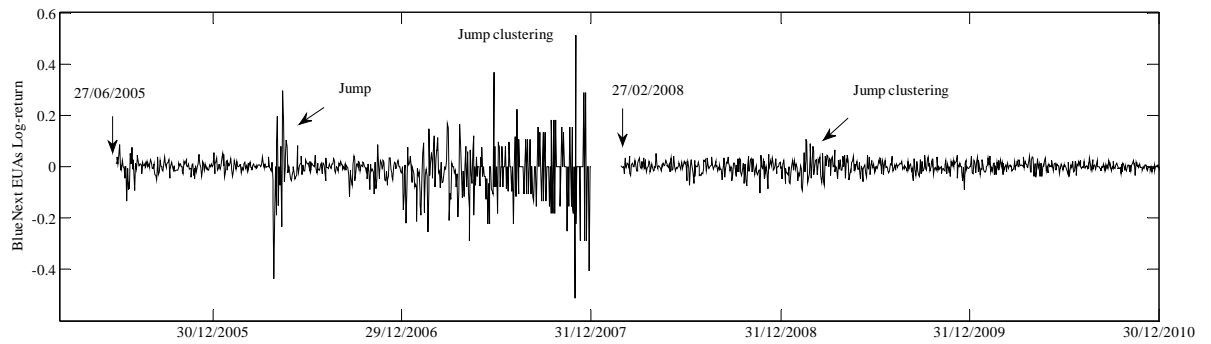
Date	Call Model	OTM	ATM	ITM	Total
In sample	$C_B(F_c)$	0.1797	0.1186	0.0383	0.0992
	$C_J(F_c)$	0.1485	0.0988	0.0355	0.0832
	$C_R(F_c, Q)$	0.1372	0.0897	0.0341	0.0765
	$C_R(F_s, Q)$	0.2079	0.1309	0.0455	0.1124
	$C_R(F_c, Q^*)$	0.0544	0.0485	0.0623	0.0566
	$C_R(F_s, Q^*)$	0.0845	0.0539	0.0371	0.0515
Out sample	$C_B(F_c)$	0.2593	0.1741	0.0863	0.1640
	$C_J(F_c)$	0.2286	0.1579	0.0862	0.1488
	$C_R(F_c, Q)$	0.2170	0.1518	0.0859	0.1430
	$C_R(F_s, Q)$	0.3103	0.2123	0.0803	0.1928
	$C_R(F_c, Q^*)$	0.1371	0.1252	0.1055	0.1190
	$C_R(F_s, Q^*)$	0.1731	0.1231	0.0571	0.1112
All	$C_B(F_c)$	0.2314	0.1495	0.0650	0.1354
	$C_J(F_c)$	0.2011	0.1322	0.0641	0.1204
	$C_R(F_c, Q)$	0.1898	0.1252	0.0634	0.1146
	$C_R(F_s, Q)$	0.2740	0.1768	0.0639	0.1574
	$C_R(F_c, Q^*)$	0.1086	0.0946	0.0848	0.0924
	$C_R(F_s, Q^*)$	0.1401	0.0944	0.0471	0.0854

Note: 1.The futures option pricing errors (RMSE) are computed for the models with the estimated parameters given in Table 4 during the period from 26/02/2008 to 30/12/2010 using the real option data. “In sample” denotes the real option data from 01/11/2010 to 30/12/2010. “Out sample” means the real option data from 03/01/2011 to 28/02/2011.

- The results are grouped into “OTM”(out-of-money,  $S/K < 0.95$ ), “ATM”(at-the-money options,  $0.95 \leq S/K \leq 1.05$ ) and “ITM”(in-of-money,  $1.05 < S/K$ ), “Total” is the pricing error (RMSE) of all options in the dataset regardless of OTM, ATM, and ITM options, respectively for the In-, Out- sample periods. “All”(all options in the dataset).
- The data are the futures options traded at ECX. Maturities are Mar-11, June-11, Sep-11and Dec-11, of 2011. The strike prices (K) are 12, 12.5, 13, 13.5, 14, 14.5, 15, and 15.5.

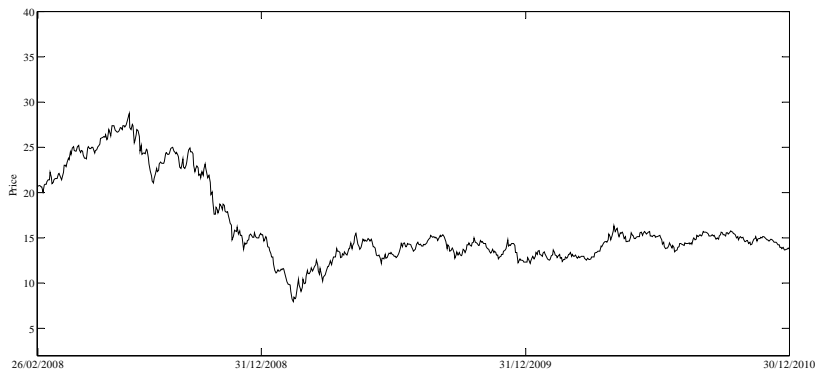


**Panel A:** The dynamics of the spot EUAs in BlueNext,

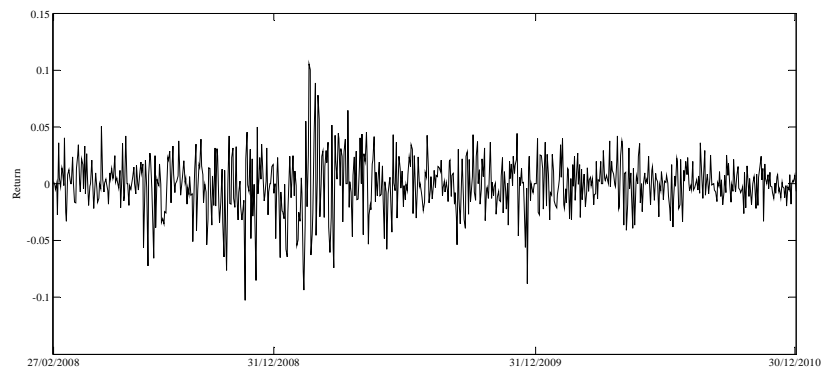


**Panel B:** The dynamics of the spot EUAs returns in BlueNext

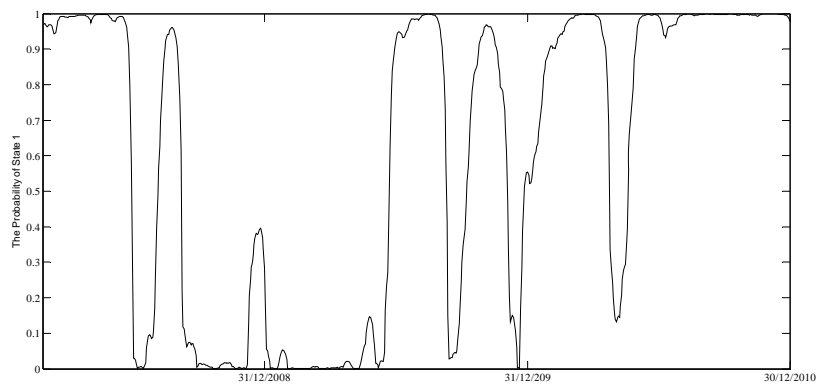
**Figure 1:** The Dynamics of Spot EUAs And Spot EUAs Returns in BlueNext



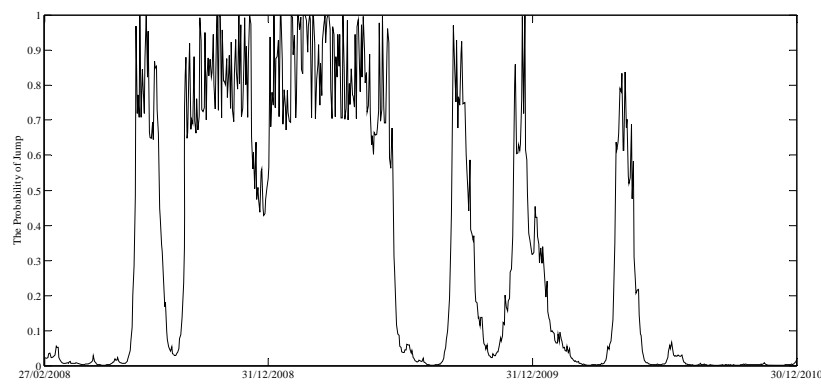
**Panel A:** The dynamics of the spot EUAs at Phase II



**Panel B:** The dynamics of the spot EUAs returns at Phase II

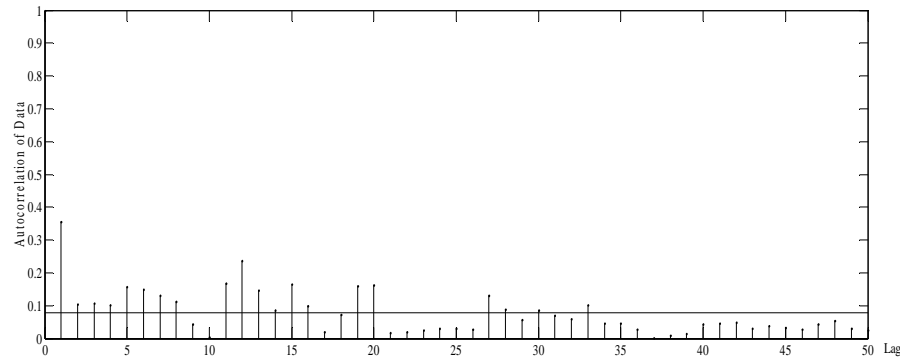


**Panel C:** The probabilistic dynamics of the low intensity with the spot EUAs returns at Phase II in BlueNext

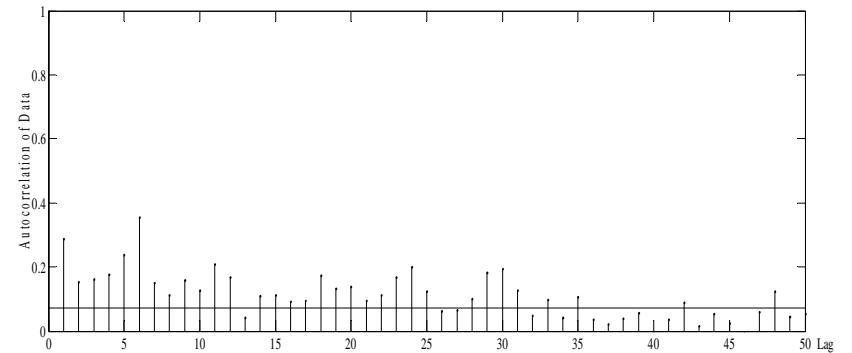


**Panel D:** The jump probabilistic dynamics with the spot EUAs return at Phase II in BlueNext

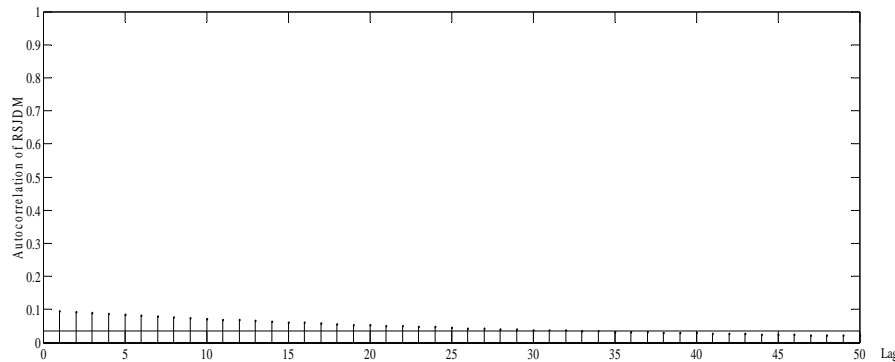
**Figure 2: The Dynamics of Spot EUAs, Its Return, The Low Intensity Probability And Jump Probability at Phase II in BlueNex**



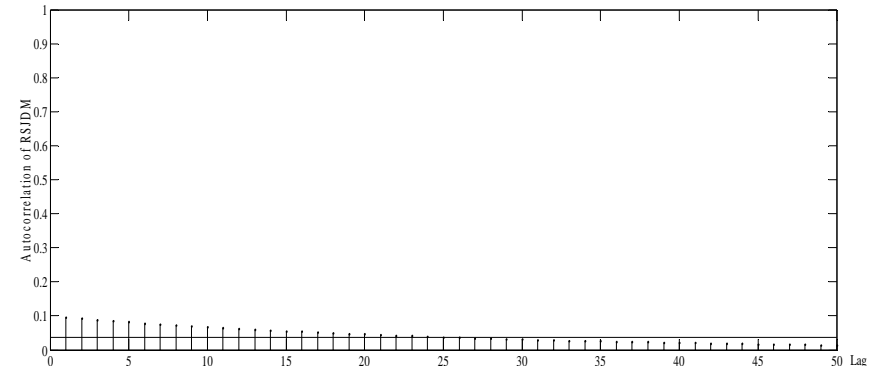
**Panel A:** The autocorrelation of squared spot EUAs returns at Phase I in BlueNext



**Panel C:** The autocorrelation of squared spot EUAs returns at Phase II in BlueNext

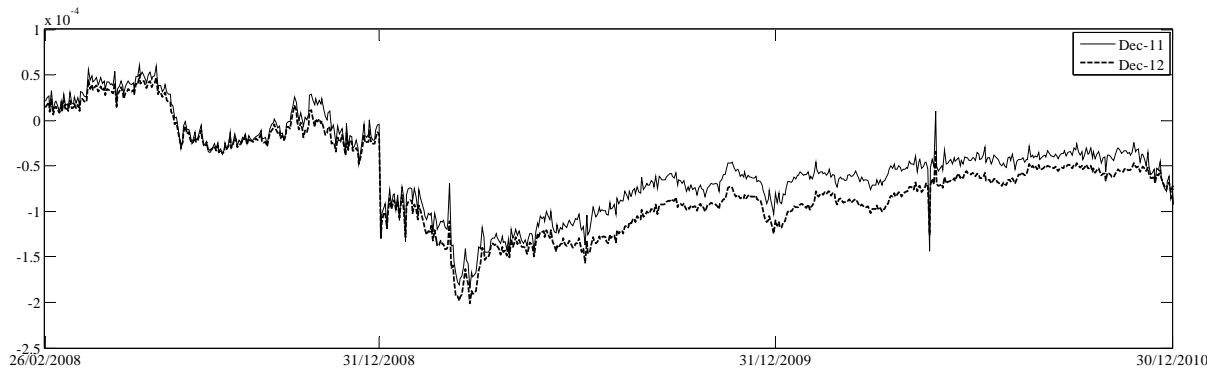


**Panel B:** The estimated autocorrelation of squared spot EUAs returns with the RSMJ model at Phase I in BlueNext



**Panel D:** The estimated autocorrelation of squared spot EUAs returns with the RSMJ model at Phase II in BlueNext

**Figure 3: The Autocorrelation and The Estimated Autocorrelation of The Spot EUAs Returns with the RSMJ Model at Phase I and II in BlueNext**



$\delta(t_k)$  denotes the daily empirical convenience yield given by (17) with during with average interest rate during the period 2008-2010.

**Figure 4: The Time Series Behavior of Convenience Yield**